Proc. Natl. Acad. Sci. USA
Vol. 96, pp. 736–741, January 1999
Neurobiology

Morphological, physiological, and biochemical changes in rhodopsin knockout mice

J. LEM*†‡, N. V. KRASNOPEROVA*, P. D. CALVERT§, B. KOSARAS¶, D. A. CAMERON‖, M. NICOLÒ*, C. L. MAKINO§, AND R. L. SIDMAN¶

*New England Medical Center, and †Departments of Ophthalmology and Genetics, Tufts University School of Medicine, Boston, MA 02111; §Department of Ophthalmology, Massachusetts Eye and Ear Infirmary, Harvard Medical School, Boston, MA 02114; ¶New England Regional Primate Research Center, Harvard Medical School, Southboro, MA 01772; and ‖Department of Physiology, Boston University School of Medicine, Boston, MA 02118

Contributed by R. L. Sidman, November 18, 1998

ABSTRACT **Mutations in rod opsin, the visual pigment protein of rod photoreceptors, account for ≈15% of all inherited human retinal degenerations. However, the physiological and molecular events underlying the disease process are not well understood. One approach to this question has been to study transgenic mice expressing opsin genes containing defined mutations. A caveat of this approach is that even the overexpression of normal opsin leads to photoreceptor cell degeneration. To overcome the problem, we have reduced or eliminated endogenous rod opsin content by targeted gene disruption. Retinas in mice lacking both opsin alleles initially developed normally, except that rod outer segments failed to form. Within months of birth, photoreceptor cells degenerated completely. Retinas from mice with a single copy of the opsin gene developed normally, and rods elaborated outer segments of normal size but with half the normal complement of rhodopsin. Photoreceptor cells in these retinas also degenerated but did so over a much slower time course. Physiological and biochemical experiments showed that rods from mice with a single opsin gene were ≈50% less sensitive to light, had accelerated flash-response kinetics, and contained ≈50% more phosducin than wild-type controls.**

Mutations in the rod photoreceptor opsin gene account for the largest proportion of inherited retinal degenerations of known genetic etiology. More than 80 mutations in the human gene have been identified (1). At early stages of disease, these mutations lead to the death of rod photoreceptors. The underlying mechanisms are not well understood. This problem has been approached by expressing mutant opsin genes in transgenic mice in the presence of the endogenous opsin gene (2–8). However, this approach caused overexpression of opsin, and it has been shown that excessive expression of normal opsin in transgenic mice leads to a degenerative phenotype (8). By expressing a mutant opsin gene in the absence of one or both native opsin genes, we should be able to isolate the molecular and physiological effects of mutant opsins from those caused by overexpression. Toward this goal, we have produced transgenic mice in which one or both copies of the opsin gene have been knocked out by targeted gene disruption. Here, we explore the impact of the loss of one or both functional alleles of opsin on the formation and physiology of rod photoreceptors.

MATERIALS AND METHODS

Targeted Disruption of the Rod Opsin Gene. A targeting construct was made from a 129SV genomic clone (Fig. 1) by using a positive–negative selection strategy. J1 embryonic stem cells (9) were electroporated with the targeting construct and selected in G418 and gancyclovir. Of 79 clones, 13 were identified as homologous recombinants by *Eco*RI digestion. In addition, six putative recombinants were verified by *Bam*HI digestion.

Assessment of Retinal-Protein Content. All animals were handled in accordance with the guidelines provided by the Association for Research in Vision and Ophthalmology. Retinas were collected from mice reared under a 14-h:10-h light:dark cycle and harvested in an ice-cold Hepes-buffered solution (130 mM NaCl/2.6 mM KCl/2.4 mM $MgCl_2$/1.2 mM $CaCl_2$/10 mM Hepes/0.02 mM EDTA, pH 7.4). Retinas were frozen immediately in liquid nitrogen and stored at −70°C until used. Frozen retinas were thawed and homogenized in a vortex mixer with hypotonic buffer containing 10 mM Tris·HCl, 2 mM DTT, 2 mM EDTA, 1 mM benzamidine, 0.1 mM phenylmethylsulfonyl fluoride, and 15 μg/ml each of aprotinin, leupeptin, and pepstatin (pH 7.4). Homogenates were solubilized in buffer containing 2% SDS and spun down at 10,000 × *g*. Samples were frozen in small aliquots at −70°C. A new aliquot was used for each experiment. Total retinal homogenates were run on SDS/12.5% polyacrylamide gels to analyze all proteins, except phosphodiesterase α-subunit (PDEα) and phosphodiesterase β-subunit (PDEβ), where 15% low cross-link gels were used (10). Retina equivalent dilutions (1/100 to 1/1000) were loaded into each lane. Proteins were transferred onto nitrocellulose membranes for 1–1.5 h, which then were blocked for 1 h at room temperature with 5% nonfat dry milk, 0.05% Tween 20 (J. T. Baker), 150 mM NaCl, and 100 mM Tris·HCl at pH 7.4. Transfer membranes were probed with primary antibodies, followed by horseradish peroxidase-conjugated secondary antibodies. Protein bands were visualized with the addition of an enhanced chemiluminescent substrate (Pierce) and exposure to MP film (Amersham). Protein bands on exposed films were scanned with a Stratagene Eagle Eye system, and band densities were quantified with Scanalytics (Billerica, MA) 2DGEL software. Calibration curves were run to determine the linear range of the method for each antibody used. The antibodies used were Ret-P1 (11) and K61–171C (12), rhodopsin; transducin α-subunit 1A (T_α1A; a gift from M. Simon, California Institute of Technology, Pasadena, CA); β636 (13) or βN1 (14), transducin β-subunit (T_β); Pat, PDEα and PDEβ (a gift from R. Lee, University of California, Los Angeles, CA); Gertie B, phosducin (15), rhodopsin kinase (a gift from R. Lefkowitz, Duke University, Durham, NC); SCT-128, arrestin (16); and P26, recoverin (17).

Difference Spectrophotometry. Mice were dark-adapted overnight. Retinas were isolated under infrared light in ice-

The publication costs of this article were defrayed in part by page charge payment. This article must therefore be hereby marked "*advertisement*" in accordance with 18 U.S.C. §1734 solely to indicate this fact.

PNAS is available online at www.pnas.org.

Abbreviations: ONL, outer nuclear layer; PDEα, phosphodiesterase α-subunit; PDEβ, phosphodiesterase β-subunit; T_α, transducin α-subunit; T_β, transducin β-subunit.

‡To whom reprint requests should be addressed. e-mail: jlem01@tufts.edu.

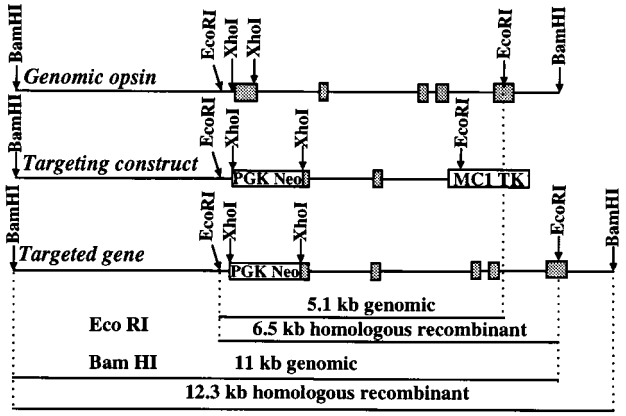

FIG. 1. The targeting construct was produced by replacing the DNA segment between the *Xho*I sites of genomic opsin with the neomycin-resistance gene (PGK Neo) and inserting the thymidine kinase gene (MC1 TK) in the second intron. Codons 1–111 were deleted in the targeted opsin gene. Desired homologous recombinants were identified by using the two restriction-digestion strategies shown at the bottom of the figure.

cold Hepes-buffered solution. Each retina was homogenized in a vortex mixer in a 1.5-ml microcentrifuge tube containing 100 μl of homogenization buffer (10 mM NaH_2PO_4/20 mM NaF/7.5 mM EDTA, pH 7.4). Under dim red light, 10 μl of each homogenate was transferred to a fresh tube containing 90 μl of 40 mM cetyltrimethylammonium chloride. An absorbance spectrum between 450 and 750 nm was taken. A second spectrum was taken after a 2-min exposure to bright light, which bleached all of the rhodopsin. The amount of rhodopsin present in each retina was calculated from the difference between the two spectra at 500 nm by using an extinction coefficient of 40,000 $M^{-1}\cdot cm^{-1}$.

Histology. Anesthetized mice were perfused through the heart with freshly prepared 2% paraformaldehyde/2.5% glutaraldehyde in 0.1 M phosphate buffer (pH 7.4) for light and electron microscopy. Eye orientation was marked by leaving a tab of lid tissue attached to the eye at the 12 o'clock position. Eyes were removed, rinsed in buffer, and immersed in 2% osmium tetroxide. During postosmication, eyes were bisected, or small calottes were removed. Specimens were dehydrated and embedded in Epon (Ted Pella, Redding, CA) by standard procedures. Sections 1 μm thick were cut and stained with alkaline toluidine blue for light microscopy. Ultrathin sections 80 nm thick were cut, stained with lead citrate and uranyl acetate, and examined with a JEOL 1200EX transmission electron microscope.

Microspectrophotometry. Mice were dark-adapted for 12–24 h and killed by cervical dislocation. Retinas were harvested under infrared illumination in medium containing 130 mM NaCl, 5.4 mM KCl, 0.8 mM $MgSO_4$, 1.0 mM $CaCl_2$, 1.0 mM Na_2HPO_4, 0.1 mM $NaHCO_3$, 5.0 mM glucose, 10.0 mM Hepes, 0.1 mg/ml BSA, 0.5 ml/100 ml MEM vitamins (100×, Sigma), 1.0 ml/100 ml MEM amino acids (50×, Sigma) at pH 7.4 (18, 19). Rods were isolated from retinal fragments by gentle chopping with a microknife and suspended in a 70-μm-thick chamber bound by two glass coverslips filled with medium. The chamber was monitored with an infrared-sensitive television camera whose output was recorded on video tape.

Absorption spectra of single rods were determined with a computer-controlled, photon-counting microspectrophotometer (20, 21). The probe beam was focused to approximate dimensions of 1×3 μm at the plane of the isolated rod outer segments. The light was polarized linearly with the plane of polarization oriented perpendicularly to the long axis of the beam. A single scan across the frequency range of 400–800 THz (750–375 nm), in 5-THz bins, was completed in less than 1 s. For each rod, three such scans were averaged. At each frequency, OD was determined as $OD = \log_{10} I_0/I_t$, where I_0 is the number of photons incident on the photomultiplier in the absence of a cell and I_t is the photon count incident on the photomultiplier after the light passed side-on through the outer segment. For I_t measurement, the probe beam, focused at 400 THz, was placed entirely within the outer-segment area of an individual rod, thus aligning the long dimension of the probe beam parallel to the long axis of the outer segment.

In some experiments, measurements were collected from large masses of rods to define the shape of the pigment's absorption spectrum. OD spectra were adjusted for baseline shifts, normalized by eye, averaged, and fitted with a frequency-dependent, eighth-order, visual pigment absorbance template $OD/OD_{max} = \Sigma a_n[(F - F_{max})/F_{max}]^n$, where F is frequency, F_{max} is frequency at the OD maximum, and coefficients a_0–a_8 were 1.0, 0.0330251, −69.2795, 182.066, 1970.61, −9017.22, −21954.1, 129796, and 75226.6. This template was derived empirically from the absorption spectra of the 11-*cis*-retinal-based visual pigment of *Bufo marinus* (marine toad) red rods, ranging from 0.83 to $1.16 \times F_{max}$ (E. F. MacNichol, G. J. Jones, and M. C. Cornwall, personal communication). After finding F_{max}, the template was used to analyze the results from individual rods, where a_0 was the free parameter of the fit. All spectra were illustrated in terms of wavelength rather than frequency.

Single-Cell Suction-Electrode Recording. Transgenic mice, aged 36–179 days, and littermate controls, aged 37–62 days, were dark-adapted overnight before an experiment. Preparation of retinal tissue and suction-electrode recording of flash responses from individual rod photoreceptors were carried out according to the method of Sung *et al.* (5), except that infrared illumination was used for all dissections. Briefly, retinas were isolated into oxygenated Leibovitz's L-15 medium and stored on ice until used. A small piece of retina was chopped finely in L-15 containing DNase I, type IV (Sigma) and loaded into a recording chamber. Tissue was perfused with bicarbonate-buffered medium (141 mM Na^+/3.6 mM K^+/2.4 mM Mg^{2+}/1.2 mM Ca^{2+}/121 mM Cl^-/20 mM HCO_3^-/10 mM glucose/10 mM Hepes/3 mM succinate/0.5 mM L-glutamate/0.02 mM EDTA/1.0 ml/50 ml of MEM amino acids (50× GIBCO/BRL)/1.0 ml/100 ml Basal Medium Eagle vitamins (100× GIBCO/BRL), pH 7.4) equilibrated with 95% O_2/5% CO_2 at 36–38°C. The outer segment of a rod was drawn into a silanized glass suction pipette that contained identical medium, except that HCO_3^- was replaced with Cl^-. Rods were stimulated with 20-ms flashes at 500 nm. Photocurrent responses were recorded with a current-to-voltage converter (Axopatch 200, Axon Instruments, Foster City, CA), low-pass filtered at 30 Hz (−3 dB, 8-pole Bessel Frequency Devices, Haverhill, MA), and digitized online at 400 Hz. No correction was made for the 16.9-ms delay introduced by low-pass filtering. Some records were also filtered digitally at 14 Hz by convolution with a Gaussian distribution (IGOR PRO software, WaveMetrics, Lake Oswego, OR).

RESULTS

Opsin-Gene Disruption. A targeting construct, deleting 15 bp upstream of the translation start site and the first 111 codons of the rod opsin gene (Fig. 1), was used to produce homologous recombinant embryonic-stem-cell clones. To produce chimeric mice, three independent recombinant clones were injected into day-3 blastocysts. As shown by Southern blot analysis of DNA prepared from offspring derived from chimeric founders, two chimeric mice produced from one embryonic-stem-cell clone gave rise to germ-line transmission (Fig. 2*A*). Wild-type (+/+), hemizygous (+/−), and homozygous (−/−) mice were produced in the expected Mendelian

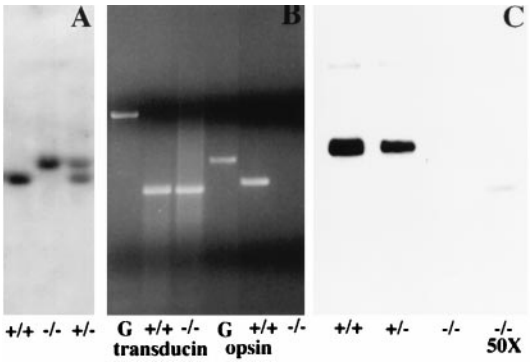

FIG. 2. (*A*) Southern blot with *Eco*RI-digested DNAs prepared from littermate animals derived from a chimeric rhodopsin knockout founder. +/+, −/−, and +/− designate wild-type, homozygous, and hemizygous mice, respectively. +/+ mice exhibit a 5.1-kb band indicative of genomic opsin DNA. −/− mice exhibit a 6.5-kb band indicative of the targeted gene. +/− mice exhibit both. (*B*) Reverse transcription–PCR. RNA prepared from retinas of 30-day-old +/+ or +/− mice were reverse transcribed and amplified with primers specific for rod T_α or rod opsin. Primer pairs spanned an intron. Although T_α mRNA was detected, no opsin mRNA was detected in −/− retinas. Transducin PCR products were 370 bp and 846 bp for RNA and DNA, respectively. Opsin PCR products were 397 bp and 513 bp for RNA and DNA, respectively. G represents amplified genomic DNA. (*C*) Western blot probed with rhodopsin-specific Ret-P1 antibody. Equivalent amounts of retinal homogenate were loaded in the first three lanes (left to right); 50-fold more homogenate was loaded in the far right lane.

proportions, indicating that the knockout was not embryonic lethal.

Rhodopsin Is Reduced in Opsin +/− Mice and Undetectable in Opsin −/− Mice. To determine whether a null opsin allele was produced, levels of opsin mRNA and protein were examined. Neither Northern blot analysis nor reverse transcription–PCR detected opsin mRNA transcripts in 4-week-old −/− mice (Fig. 2*B*). Opsin-protein levels in whole retinal homogenates were measured with two methods: scanning densitometry of Western blots and bleaching difference spectrophotometry. In a given Western analysis, −/−, +/−, and +/+ control mice were age-matched littermates. We studied five independent animal sets, ranging in age from 23 to 55 days. Results were similar in this age span; the level of rhodopsin in +/− mice was ≈57% of that in +/+ controls and was undetectable in −/− retinas (Fig. 2*C*). Difference spectra of whole retinal homogenates from three separate sets of littermate +/− and +/+ animals at 4, 10, and 24 weeks confirmed that +/− retinas had ≈50% of the normal amount of rhodopsin (Fig. 3*A*).

At 4, 10, and 24 weeks, the lengths of +/+ and +/− rod outer segments differed by less than 10% (see below). To determine whether the decrease in rhodopsin was caused by a reduction in the number of outer segments or by a decrease in the rhodopsin concentration in each cell, rods were examined microspectrophotometrically. The specific density [OD at λ_{max} divided by outer segment diameter] of individual +/+ rods was 0.012 ± 0.022 μm^{-1} (mean ± SD, $n = 30$; Fig. 3*C*), similar to that of photoreceptors from other vertebrates (22–24). In contrast, the specific density of +/− rods was 0.006 ± 0.012 μm^{-1} ($n = 32$; Fig. 3*C*), a significantly lower value ($P < 0.03$). The outer-segment diameters (i.e., path lengths) in +/+ and +/− mice were the same; 1.4 ± 0.2 μm for both. Thus, the concentration of rhodopsin molecules within single rods from +/− mice was ≈50% of normal.

Absorption spectra of large masses of overlapping rods from +/+ and +/− mice were similar and were consistent with the presence of a single 11-*cis*-retinal-based pigment with λ_{max} at 505 nm. There was no indication of the presence of any pigment other than rhodopsin (Fig. 3*B*).

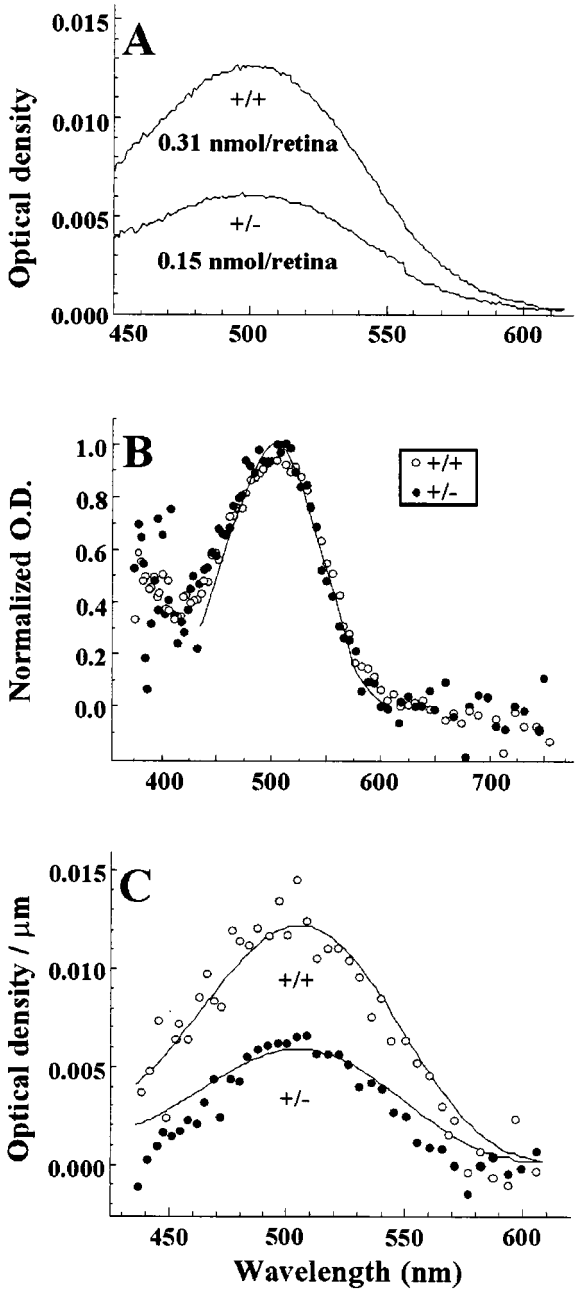

FIG. 3. (*A*) Difference spectra of retinal extracts. +/− retinal homogenates have approximately half the rhodopsin content of age-matched (4 week) +/+ retinas. (*B*) Normalized mean absorption spectra of rod masses from +/+ (open circles; $n = 6$) and +/− (closed circles; $n = 5$) mice. Fitting the template to the +/+ spectrum yielded an absorption peak (λ_{max}) of ≈505 nm. (*C*) Microspectrophotometric analysis of single rods. The OD spectrum for each rod was divided by the width (in μm) of the rod's outer segment. Circles plot the mean specific absorbance values for 30 +/+ rods (open circles) and 32 +/− rods (closed circles). The lines show the template in *B*, scaled to fit the +/+ and +/− results.

Retinal Morphology. Retinal morphology of hemizygous and homozygous knockout mice and age-matched littermate controls at 15, 30, and 90 days of age were examined. For each age, two or three animals of each type were analyzed, unless otherwise indicated. Because the mouse retinal ONL is comprised of 95% rod and 5% cone nuclei, the thickness of the ONL provides an estimate of the number of rods present. ONL

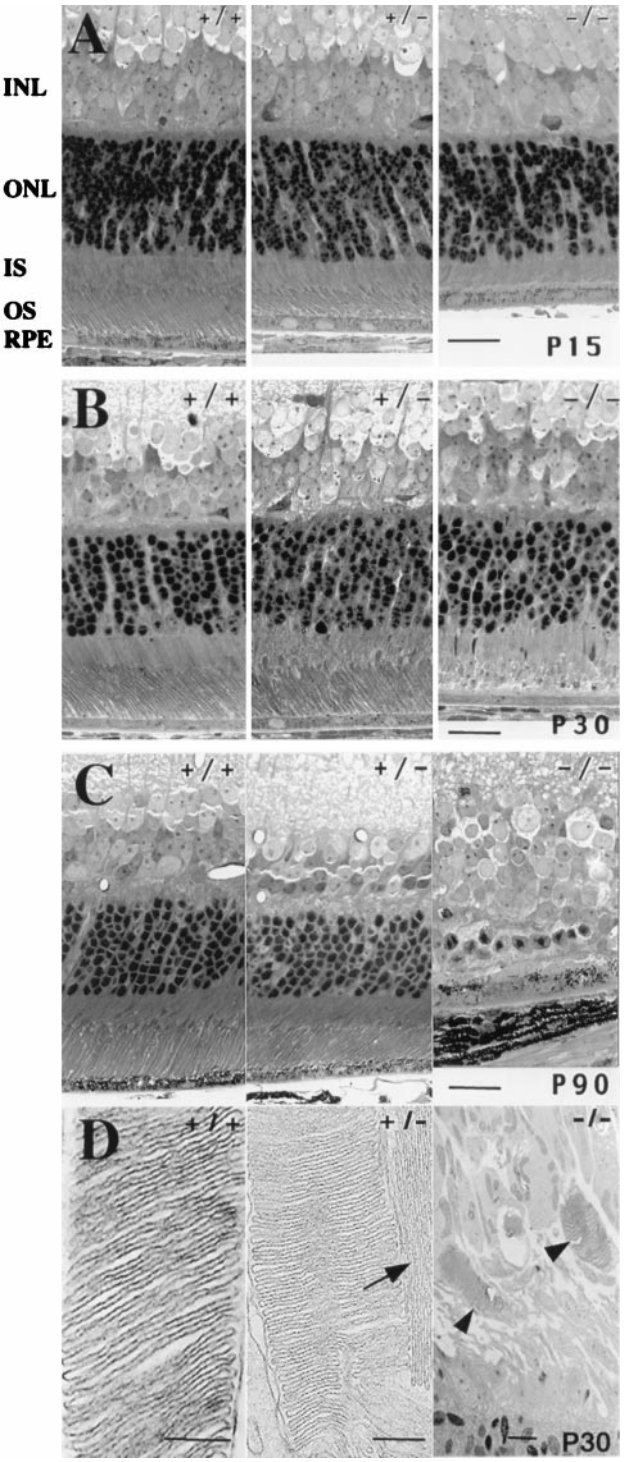

FIG. 4. Retinal morphology. Light microscopy shows retinas of 15-day-old (*A*), 30-day-old (*B*), and 90-day-old (*C*) animals (*Left*, +/+ littermate mice; *Center*, +/− littermate mice; *Right*, −/− littermate mice). INL, inner nuclear layer; ONL, outer nuclear layer; IS, inner segments; OS, outer segments; RPE, retinal pigmented epithelium. (Bar = 20 μm.) (*D*) Electron micrographs were prepared from the same tissue blocks used for light microscopy. The arrow indicates abnormally oriented membranes. Arrowheads point to outer segments in the −/− retina. (Bar = 200 nm for +/+ and +/−; bar = 1 μm for −/−.)

thicknesses of 15-day −/−, +/−, and +/+ retinas were comparable at 10–12 rows of nuclei (Fig. 4*A*). However, photoreceptor outer segments were absent in −/− retinas and were at ≈50% shorter in +/− retinas, relative to wild-type controls. No other gross defects in eye structure were observed.

By 30 days, the ONL of +/− and +/+ retinas were at maximal thickness, and +/− outer segments were nearly normal in length (Fig. 4*B*). In −/− mouse retinas, increased numbers of darkly staining pyknotic cells were clearly evident, and ONL thickness was decreased by one or two rows. Rod outer segments were missing, as observed at earlier ages. Darkly staining condensations distal to the inner segments were apparent.

ONL thickness was reduced by one or two rows in 90-day +/− retinas, and outer-segment length was shortened slightly (Fig. 4*C*). In the −/− retina, degeneration was nearly complete. Cone cells comprised most of the single, fragmented row of nuclei that remained of the ONL. The prominent condensations observed in the 30-day −/− retina were no longer found.

Although misoriented outer-segment membranes were observed at the electron-microscopic level, rods from 30-day +/− retinas generally appeared to have properly oriented and spaced disk membranes (Fig. 4*D*). Retinas from −/− mice exhibited very few outer segments, and those present were greatly shortened (Fig. 4*D*).

Single-Cell Recordings. In single-cell suction-electrode recordings, bright flashes elicited responses of similar amplitude in +/+ and +/− rods (Table 1). However, +/− rods responded to dim flashes with reduced sensitivity (Fig. 5 *B* and *C*). On average, a flash of 69 photons·μm^{-2} at 500 nm elicited a half-maximal response in +/+ rods, whereas in +/− rods, 118 photons·μm^{-2} were required. Outer-segment length and diameter were similar in the transgenic and control rods recorded. Thus, the lower sensitivity of transgenic rods was attributed to a diminished quantal catch caused by the decreased intracellular rhodopsin concentration, consistent with the microspectrophotometric results.

There were also differences in photoresponse kinetics (Fig. 5 *A* and *B*; Table 1). At subsaturating flashes, responses of +/− rods peaked and recovered sooner than those of +/+ controls. The faster recovery of +/− rod responses was manifested by a reduction in integration time, defined as the integral of the response divided by the response amplitude. −/− rods failed to develop outer segments and were not analyzed.

Secondary Effects on the Expression Level of Other Phototransduction Proteins. The accelerated recovery time of the light response suggested that one or more phototransduction proteins besides rhodopsin might have changed in +/− mice. To examine this possibility, levels of eight additional phototransduction proteins were quantified by scanning densitometry of Western blots. Whole retinal homogenates from littermate −/−, +/−, and +/+ mice 23 to 183 days of age were used (Fig. 6*A*). +/− mice essentially had wild-type levels of T_α ($n = 5$), T_β ($n = 6$), PDEα ($n = 5$), PBEβ ($n = 5$), rhodopsin kinase ($n = 5$), arrestin ($n = 6$), and recoverin ($n = 6$). In contrast, phosducin ($n = 4$) was increased significantly by ≈50% relative to wild-type levels (Fig. 6*B*).

In −/− mice 30- to 70-days old, levels of T_α ($n = 5$), T_β ($n = 4$), PDEα ($n = 4$), PDEβ ($n = 4$), rhodopsin kinase ($n = 2$), arrestin ($n = 2$), and recoverin ($n = 2$) were reduced significantly. Phosducin (23–30 days, $n = 2$) protein approached wild-type levels (Fig. 6*B*). All proteins dropped to undetectable levels in animals 141 days and older, as rod cells completely degenerated.

DISCUSSION

Mice with a null mutation of the rod opsin gene have been produced. Retinas from −/− mice lacked rod opsin mRNA and protein. Rhodopsin was present in +/− rods but at half the normal concentration. There were several changes in the

Table 1. Flash response parameters

Genotype	Sensitivity i_0, photons·μm^{-2}	Dim-flash-response kinetics		Maximal response r_{max}, pA
		t_p, ms	t_i, ms	
+/+	69 ± 40 (10)	140 ± 20 (10)	270 ± 70 (10)	9 ± 3 (10)
+/−	118 ± 50 (16)	120 ± 10 (16)	190 ± 50 (16)	10 ± 2 (16)
Significance	$P < 0.02$	$P < 0.01$	$P < 0.006$	

Values are given as mean ± SD; number of measurements are given in parentheses. Significance was evaluated with Student's *t* test. Abbreviations: i_0, the flash strength at 500 nm producing a half-maximal response; t_p, the time interval from the flash to the response peak; t_i, the area of the response divided by its peak amplitude; r_{max}, the maximal saturating response amplitude.

properties of the electrical responses to light in +/− rods. Sensitivity to light was reduced twofold, consistent with the decreased rhodopsin density. The decreased light sensitivity of human carriers of null mutations in rhodopsin may have a similar basis (25). Flash responses of +/− rods had faster kinetics than normal, suggesting that changes in the activities of proteins mediating photoresponse recovery had occurred.

With photon absorption, rhodopsin induces the exchange of GTP for GDP bound to transducin, causing it to dissociate into T_α-GTP and $T_{\beta\gamma}$. T_α-GTP relieves inhibition on PDE, which hydrolyzes cGMP, leading to closure of cation-permeable channels in the plasma membrane. In response recovery, rhodopsin shuts off after phosphorylation by rhodopsin kinase and subsequent binding to arrestin; T_α-GTP activity is quenched after it hydrolyzes its GTP; cGMP levels are restored, and the channels in the plasma membrane reopen (26). Acceleration of any of these processes could lead to faster response recovery.

As a first step toward elucidating the mechanism mediating changes in photoresponse recovery, the levels of phototransduction proteins were measured. Levels of T_α, T_β, PDEα, PDEβ, rhodopsin kinase, arrestin, and recoverin, a protein that regulates rhodopsin kinase activity, were essentially normal in +/− mice. Phosducin was elevated by 50%. *In vitro*, phosducin binds $T_{\beta\gamma}$ with high affinity, thereby regulating its availability to bind T_α (14, 27–29). However, it is unclear how phosducin could account for the accelerated response kinetics in +/− mice. First, phosducin may not be elevated in rod outer segments, because the phosducin level was normal in young −/− mice lacking outer segments. Second, if a complete quenching of T_α depends on its reunion with $T_{\beta\gamma}$ (30), then, given that levels of T_β in +/− mice were unchanged, an

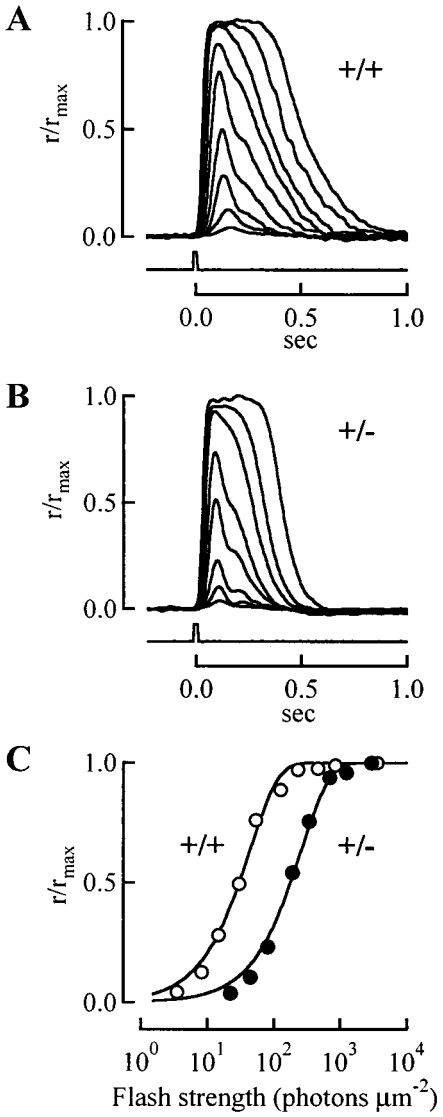

FIG. 5. Averaged responses of +/+ rods (*A*) and +/− rods (*B*) to 500-nm flashes of increasing strength. Responses are normalized to maximal response amplitudes (18 pA for the +/+ rod and 12 pA for the +/− rod). Traces underneath are signals from flash monitors. Photoresponse recovery is faster in the +/− rod. (*C*) Normalized response amplitudes from *A* and *B* plotted against flash strength. Lines show fit of the data to a saturating exponential: $r/r_{max} = 1 - e^{-ki}$, where i is the flash strength, $k = \ln(2/i_0)$, and i_0 is the flash strength giving rise to a half-maximal response. For the +/+ rod, i_0 was 30.6 photons·μm^{-2}; for the +/− rod, i_0 was 182 photons·μm^{-2}.

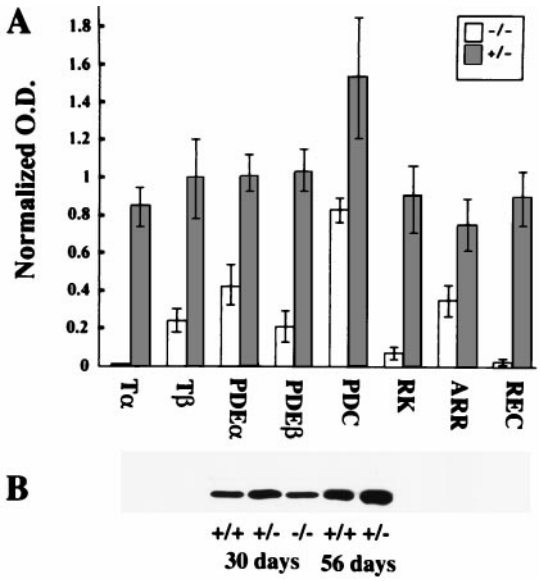

FIG. 6. (*A*) Levels of T_α, T_β, PDEα, PDEβ, phosducin (PDC), rhodopsin kinase (RK), arrestin (ARR), and recoverin (REC) in −/− (open bars) and +/− (gray bars) mice normalized to +/+ values (mean ± SD). (*B*) This Western blot with equal amounts of retinal homogenate from +/+, +/−, and −/− mice at 30 and 56 days of age was probed with phosducin antibody.

increased ratio of phosducin to $T_{\beta\gamma}$ might be predicted to delay rather than accelerate photoresponse recovery. Further studies are required to determine the basis for the accelerated response kinetics and any effects of elevated phosducin.

Opsin-gene disruption also affected rod morphology and development. At 15 days, −/− retinas contained normal numbers of rod nuclei with inner segments, but outer segments failed to develop. By 30 days, 10–15% of rod nuclei were lost, and at 90 days, over 90% were lost. Hence, the complete absence of rhodopsin had severe effects on normal rod outer-segment development and rod-cell viability. Humphries *et al.* (31) reported similar histological changes in a different rhodopsin knockout mouse line.

Fruit flies with a null rhodopsin mutation showed corresponding histological deficits. Rhabdomeres, the functional equivalent of vertebrate rod outer segments, formed initially but failed to mature (32). In our 30-day −/− mice, a few greatly shortened outer segments were detected at the electron-microscopic level. However, these were likely to be cone outer segments, because electroretinography indicated normal cone function at this age (K. Reuther, J. Frederick, and W. Baehr, personal communication). Our inability to detect any outer segments at 90 days of age implies that cone homeostasis also was compromised. This finding could explain why Humphries *et al.* (31) observed reduced cone electroretinographic responses in their rhodopsin knockout mice at 7 weeks of age and why a human with autosomal recessive retinitis pigmentosa caused by null mutations in both rod opsin alleles gave barely discernable cone electroretinographic responses to white flickering light (25).

In hemizygous rod opsin knockout mice, early photoreceptor outer-segment development was retarded. At 15 days, rod outer-segment length was about half that of wild-type, but as the +/− mice matured, outer segments extended to approximately normal lengths. However, before any significant retinal degeneration occurred, the rhodopsin content of individual +/− rod outer segments was diminished by half. Older +/− animals exhibited a very slow retinal degeneration. By 90 days of age, one or two rows of photoreceptor nuclei had been lost, and there was a slight reduction in outer-segment lengths of the remaining rods. These results suggest that there is a lower as well as an upper limit to the amount of rhodopsin required for rod survival. The lower limit must lie near 50% of normal levels.

We thank R. Lee for antibodies to phosducin, T_{β}, PDEα, and PDEβ, P. Hargrave and C. Barnstable for rhodopsin antibodies, M. Simon for T_{α} antibody, R. Lefkowitz for rhodopsin kinase antibody, W. C. Smith for arrestin antibody, A. Dizhoor for recoverin antibody, and J. Dausman, M. Applebury, and M. C. Cornwall for helpful discussions. This work was supported by National Institutes of Health Grants EY12008 (to J.L.), EY11160 (to D.A.C.), EY06857 (to P.D.C.), and EY06631 (to R.L.S.), as well as grants from the Foundation Fighting Blindness (to J.L.), Research to Prevent Blindness (to J.L. and C.L.M.), Fight-for-Sight (to J.L.), the E. Mathilde Ziegler Fund (to C.L.M.), the Lions of Massachusetts (to C.L.M. and J.L.), and the Milton Fund (to C.L.M.).

1. Gal, A., Apfelstedt-Sylla, E., Janecke, A. R. & Zrenner, E. (1997) *Prog. Retin. Eye Res.* **16,** 51–79.
2. Chen, J., Makino, C. L., Peachey, N. S., Baylor, D. A. & Simon, M. I. (1995) *Science* **267,** 374–377.
3. Li, T., Franson, W. K., Gordon, J. W., Berson, E. L. & Dryja, T. P. (1995) *Proc. Natl. Acad. Sci. USA* **92,** 3551–3555.
4. Li, T., Snyder, W. K., Olsson, J. E. & Dryja, T. P. (1996) *Proc. Natl. Acad. Sci. USA* **93,** 14176–14181.
5. Sung, C.-H., Makino, C., Baylor, D. & Nathans, J. (1994) *J. Neurosci.* **14,** 5818–5833.
6. Naash, M. I., Hollyfield, J. G., Al-Ubaidi, M. R. & Baehr, W. (1993) *Proc. Natl. Acad. Sci. USA* **90,** 5499–5503.
7. Huang, P. C., Gaitan, A. E., Hao, Y., Petters, R. M. & Wong, F. (1993) *Proc. Natl. Acad. Sci. USA* **90,** 8484–8488.
8. Olsson, J. E., Gordon, J. W., Pawlyk, B. S., Roof, D., Hayes, A., Molday, R. S., Mukai, S., Cowley, G. S., Berson, E. L. & Dryja, T. P. (1992) *Neuron* **9,** 815–830.
9. Li, E., Bestor, T. H. & Jaenisch, R. (1992) *Cell* **69,** 915–926.
10. Baehr, W., Devlin, M. J. & Applebury, M. L. (1979) *J. Biol. Chem.* **254,** 11669–11677.
11. Fekete, D. M. & Barnstable, C. J. (1983) *J. Neurocytol.* **1983,** 785–803.
12. Adamus, G., Zam, Z. S., Arendt, A., Palczewski, K., McDowell, J. H. & Hargrave, P. A. (1991) *Vision Res.* **31,** 17–31.
13. Lee, R. H., Lieberman, B. S., Yamane, H. K., Bok, D. & Fung, B. K.-K. (1992) *J. Biol. Chem.* **267,** 24776–24781.
14. Xu, J., Wu, D., Slepak, V. Z. & Simon, M. I. (1995) *Proc. Natl. Acad. Sci. USA* **92,** 2086–2090.
15. Lee, R. H., Whelan, J. P., Lolley, R. N. & McGinnis, J. F. (1988) *Exp. Eye Res.* **46,** 829–840.
16. Smith, W. C. (1996) *Exp. Eye Res.* **62,** 585–592.
17. Dizhoor, A. M., Ray, S., Kumar, S., Niemi, G., Spencer, M., Brolley, D., Walsh, K. A., Philipov, P. P., Hurley, J. B. & Stryer, L. (1991) *Science* **251,** 915–918.
18. Leibovic, K. N. (1986) *J. Neurosci. Methods* **15,** 301–306.
19. Robinson, D. W., Ratto, G. M., Lagnado, L. & McNaughton, P. A. (1993) *J. Physiol.* **462,** 465–481.
20. MacNichol, E. F., Jr. (1978) in *Frontiers of Visual Science*, eds. Cool, S. J. & Smith, E. L., III (Springer, Berlin), pp. 194–208.
21. Levine, J. S. & MacNichol, E. F., Jr. (1985) in *The Visual System*, eds. Fein, A. & Levine, J. S. (Liss, New York), pp. 73–78.
22. Bowmaker, J. K., Dartnall, H. J. A., Lythgoe, J. N. & Mollon, J. D. (1978) *J. Physiol.* **274,** 329–348.
23. Cameron, D. A., Cornwall, M. C. & MacNichol, E. F., Jr. (1997) *J. Neurosci.* **17,** 917–923.
24. Hàrosi, F. I. (1975) *J. Gen. Physiol.* **66,** 357–382.
25. Rosenfeld, P. J., Cowley, G. S., McGee, T. L., Sandberg, M. A., Berson, E. L. & Dryja, T. P. (1992) *Nat. Genet.* **1,** 209–213.
26. Bownds, M. D. & Arshavsky, V. Y. (1995) *Behav. Brain Sci.* **18,** 415–424.
27. Bauer, P. H., Müller, S., Puzicha, M., Pippig, S., Obermaier, B., Helmreich, E. J. M. & Lohse, M. J. (1992) *Nature (London)* **358,** 73–76.
28. Lee, R. H., Lieberman, B. S. & Lolley, R. N. (1987) *Biochemistry* **26,** 3983–3990.
29. Yoshida, T., Willardson, B. M., Wilkins, J. F., Jensen, G. J., Thornton, B. D. & Bitensky, M. W. (1994) *J. Biol. Chem.* **269,** 24050–24057.
30. Yamazaki, A., Hayashi, F., Tatsumi, M., Bitensky, M. W. & George, J. S. (1990) *J. Biol. Chem.* **265,** 11539–11548.
31. Humphries, M. M., Rancourt, D., Farrar, G. J., Kenna, P., Hazel, M., Bush, R. A., Sieving, P. A., Sheils, D. M., McNally, N., Creighton, P., *et al.* (1997) *Nat. Genet.* **15,** 216–219.
32. Kumar, J. P. & Ready, D. F. (1995) *Development (Cambridge, U.K.)* **121,** 4359–4370.